



Superconducting Phase at 7.7 K in the Hg_xReO_3 Compound with a Hexagonal Bronze Structure

Kenya Ohgushi,^{1,2,3} Ayako Yamamoto,^{2,3} Yoko Kiuchi,¹ Chandreyee Ganguli,¹ Kazuyuki Matsubayashi,^{1,2}
Yoshiya Uwatoko,^{1,2} and Hidenori Takagi^{2,3,4}

¹*Institute for Solid State Physics, University of Tokyo, Kashiwa, Chiba 277-8581, Japan*

²*JST, TRIP, Chiyoda, Tokyo 102-0075, Japan*

³*Advanced Science Institute, RIKEN, Wako, Saitama 351-0198, Japan*

⁴*Department of Advanced Materials, University of Tokyo, Kashiwa, Chiba 277-8561, Japan*

(Received 16 June 2010; revised manuscript received 1 September 2010; published 4 January 2011)

We have successfully synthesized a new rhenium-based hexagonal bronze material, Hg_xReO_3 , which exhibits superconductivity with the transition temperature $T_c = 7.7$ K at ambient pressure and 11.1 K at 4 GPa. This compound is a superconductor with the highest T_c among hexagonal bronzes. Moreover, it presents the novel crystallographic feature that $(\text{Hg}_2)^{2+}$ polycations, in contrast to monatomic cations in known hexagonal bronzes, are incorporated into open channels. There is evidence that conducting electrons tightly couple with Hg-related phonons. Our results inspire detailed studies on the role of the rattling phonon in the occurrence of superconductivity in the hexagonal bronzes.

DOI: 10.1103/PhysRevLett.106.017001

PACS numbers: 74.10.+v, 74.25.Dw, 74.25.Kc

Hexagonal tungsten bronzes with the chemical formula $A_x\text{WO}_3$ make up a classical family of superconductors [1–3]. The crystal structure (space group $P6_3/mcm$) shown in Fig. 1(a) can be viewed as consisting of a WO_3 framework with A cations in the open channels [4]. The framework is composed of corner-shared WO_6 octahedra, which lead to linear chains along the c axis and kagome networks in the a - b plane. Since the W-O-W bond is bent in the a - b plane, electrons can hardly move in this plane, forming quasi one-dimensional Fermi surfaces [5,6]. A hexagonal tunnel running along the c axis can accommodate monovalent ions such as Li^+ , K^+ , Rb^+ , Cs^+ , In^+ , and Tl^+ , as well as divalent ions such as Ca^{2+} , Sr^{2+} , Ba^{2+} , Sn^{2+} , and Pb^{2+} . Most of these cations are located at the center of a hexagonal prism, and thus are coordinated by 12 oxygens [Fig. 1(b)]. When this site is fully occupied, the x value becomes $1/3$. On the other hand, a K^+ ion with a small ionic radius prefers a lower number coordination, and is displaced to an off-center site as shown in Fig. 1(c) [7]. A similar off-center displacement occurs when $A = \text{In}$, Tl , and Pb , where a stereochemical active lone pair ($6s^2$ electrons) drives a distorted metal coordination [8,9]. In these cases, one of the two split sites is occupied, maintaining a stoichiometric composition $x = 1/3$.

Irrespective of the valence and position of the A cation, many hexagonal tungsten bronzes commonly undergo superconducting transitions at a low temperature. The highest transition temperature (T_c) reported to date is 7.5 K in $\text{Rb}_{0.26}\text{WO}_3$, which was initially discovered in 1965 [1,10]. T_c is extremely sensitive to material parameters, such as the A cation species and composition x [10,11], and there seems to be no guiding principle for raising T_c . However, there is a valuable clue in that an isostructural rhenium compound $\text{K}_{0.3}\text{ReO}_3$ is a superconductor with $T_c = 3.6$ K [12], inferring that superconductivity is a prevailing phenomenon even

in nontungsten hexagonal bronzes. In this Letter, we report superconductivity with $T_c = 7.7$ K in the hexagonal rhenium bronze $\text{Hg}_{0.44}\text{ReO}_3$. This compound uniquely contains $(\text{Hg}_2)^{2+}$ polycations within open tunnels, and we argue a possibility that the phonons associated with $(\text{Hg}_2)^{2+}$ polycations are relevant to the high T_c .

Polycrystalline Hg_xReO_3 was synthesized by using a cubic-anvil-type high-pressure apparatus. The starting materials HgO and ReO_2 were mixed in the molar ratio 1:1, and were placed in an Au capsule [13]. This was loaded into a pyrophyllite cube, and pressed to 4 GPa. It was heated up to 873 K for 15 minutes. Powder x-ray diffraction using $\text{Cu } K_\alpha$ radiation indicated a small impurity phase such as HgReO_4 and ReO_2 . Hg droplets were also observed. The HgReO_4 and Hg could be removed by washing with water and by a mechanical process, respectively. The Hg concentration x was determined by a

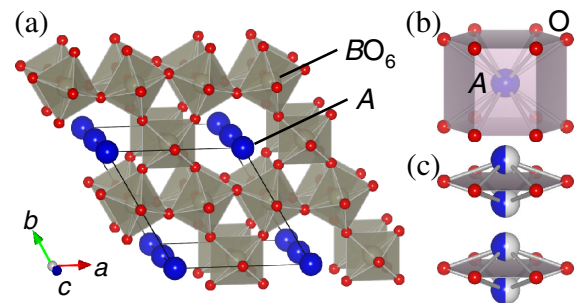


FIG. 1 (color online). (a) Crystal structure of hexagonal bronze $A_{1/3}\text{BO}_3$. The solid line shows a primitive unit cell. (b) Coordination environment of an A cation when the atomic position is $2b$ (0, 0, 0). The A cation is surrounded by 12 oxygens. (c) Coordination environment of an A cation when the atomic position is $4e$ (0, 0, z) with $z = 0.125$. An A site is split into two off-centered sites.

scanning electron microscope equipped with an energy-dispersive x-ray spectrometer. Most electronic properties were investigated for as-grown pellets, whereas the specific heat and magnetic susceptibility in the normal state were measured for pressed powders after removing the impurity phases. The data at ambient pressure were collected using a commercial setup (Quantum Design, PPMS and MPMS). The resistivity measurements under high pressure were performed with a cubic-anvil-type apparatus, using glycerine and pyrophyllite as the pressure-transmitting medium [14].

Energy-dispersive x-ray spectroscopy for Hg_xReO_3 gives the apparently anomalous result that $x = 0.44(7)$, which greatly exceeds the stoichiometric value $1/3$. This paradox can be resolved by assuming that the Hg atoms simultaneously occupy two off-centered sites, and that there is an Hg deficiency from the stoichiometric composition $x = 2/3$. We performed the Rietveld refinement of the x-ray diffraction profile [Fig. 2(a)] on the basis of this model [15], where the isotropic atomic displacement parameters for Re and O were fixed at typical values, $B(\text{Re}) = 4 \times 10^{-3} \text{ nm}^2$ and $B(\text{O}) = 1 \times 10^{-2} \text{ nm}^2$. We note here that the occupancy for Hg was set to be $g(\text{Hg}) = 0.66$ according to the chemical analysis. The agreement between the refinement pattern and the

experimental pattern is fairly good; the reliability indices are $R_{\text{wp}} = 22.1\%$ and $S = 1.32$. This analysis yields an averaged crystal structure with lattice constants $a = 0.7366(1) \text{ nm}$ and $c = 0.7506(1) \text{ nm}$, and atomic positions: Hg $4e$ [0, 0, 0.131(1)]; Re $6g$ [0.499(3), 0, 1/4]; O1 $12j$ [0.408(3), 0.204(3), 1/4]; and O2 $6f$ (1/2, 0, 0). The isotropic atomic displacement parameter for Hg is $B(\text{Hg}) = 0.118(3) \text{ nm}^2$. Part of the obtained structure is visualized in Fig. 2(b), which is interpreted as follows: one $(\text{Hg}_2)^{2+}$ polycation formed by two Hg^+ ions at two off-centered sites is incorporated into a hexagonal prism. This view is plausible, since an Hg^+ ion with one $6s$ electron has a strong tendency to form a metal-metal bond with another Hg^+ ion. The observed Hg–Hg distance of the intra $(\text{Hg}_2)^{2+}$ polycation, 0.198 nm, is slightly shorter than the averaged Hg–Hg distance of about 20 oxides in literature, 0.250 nm [16]. This suggests that the Hg–Hg bond has a potential tendency to expand. On the other hand, the Hg–Hg distance of the inter $(\text{Hg}_2)^{2+}$ polycation is quite short, 0.178 nm, leading to strong Coulomb repulsion between two adjacent molecules [Fig. 2(c)]. To relax such a tightly stuffed condition, nature prefers to extract some of the Hg^+ ions from the tunnels; this is why there are Hg deficiencies in Hg_xReO_3 . Even though each Hg^+ ion can independently be deficient in our analysis, we speculate that there is a considerable number of $(\text{Hg}_2)^{2+}$ polycation deficiencies due to a strong metal-metal bond. The Hg^+ ion located adjacent to a vacancy probably shifts toward the vacant site, making the metal-metal bond length more regular [Fig. 2(d)]. These considerations hint that $(\text{Hg}_2)^{2+}$ polycations are loosely linked to ReO_3 frameworks.

Figure 3(a) represents the electrical resistivity of $\text{Hg}_{0.44}\text{ReO}_3$, which exhibits metallic conduction due to the $\text{Re}^{5.56+}$ ions with $(5d)^{1.44}$ electronic configurations. The resistivity drops to zero at low temperature (T), indicating the onset of superconductivity. The Meissner signal [Fig. 3(b)] indicates that this superconductivity has a bulk nature (the volume fraction being 200% at 1.8 K). The T_c estimated from the midpoint of the resistivity drop is 7.7 K, which, to the best of our knowledge, is the highest T_c among the known hexagonal bronze superconductors. The specific heat (C) presented in Fig. 3(c) does not show a discontinuous jump at T_c , which is likely related to the experimental precision or the broadened nature of the transition due to Hg deficiencies. The C/T , however, goes to zero at the low T limit, supporting the concept that all the electrons participate in forming the Cooper pairs. Figure 3(d) shows the resistivity scaled by the 16 K value under pressure. The T_c shows a nonmonotonic pressure dependence [inset of Fig. 3(d)]: upon applying pressure, T_c rapidly rises, reaching a maximum value of 11.1 K at about 4 GPa, and then gradually decreases.

We investigated the phase diagram in the magnetic field-temperature (H - T) plane. Figure 4(a) represents resistivity as a function of H . The upper critical field (H_{c2}) was

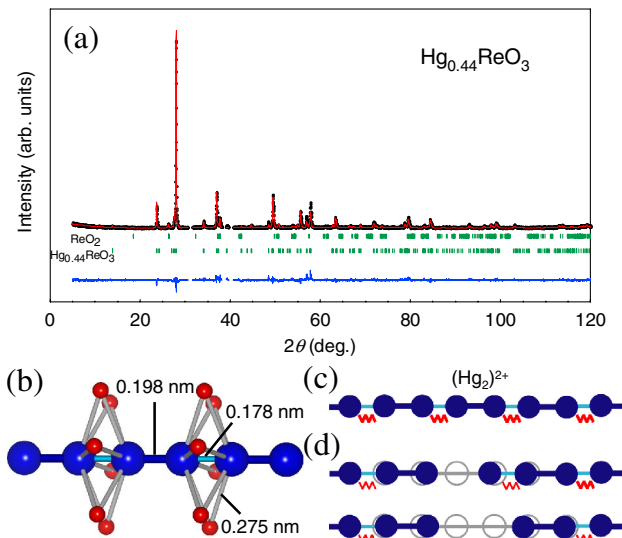


FIG. 2 (color online). (a) Rietveld refinement of x-ray diffraction profiles for $\text{Hg}_{0.44}\text{ReO}_3$. The black dots and solid (red) line represent the observed and calculated intensities, respectively. The solid (blue) line at the bottom of the panel is the difference between them. The tick (green) marks at the middle of the panel are the positions of Bragg reflections for $\text{Hg}_{0.44}\text{ReO}_3$ and ReO_2 . (b) Hg–Hg and Hg–O bond lengths deduced from the Rietveld analysis. The thick (blue) bond indicates a metal–metal bond formed by two Hg^+ ions. (c) A network of Hg atoms without vacancies. Adjacent $(\text{Hg}_2)^{2+}$ polycations strongly repel each other. (d) A network of Hg atoms with an Hg^+ (upper) and $(\text{Hg}_2)^{2+}$ (lower) vacancy. Hg^+ ions are expected to shift slightly toward the vacant site, resulting in a regular metal–metal bond length.

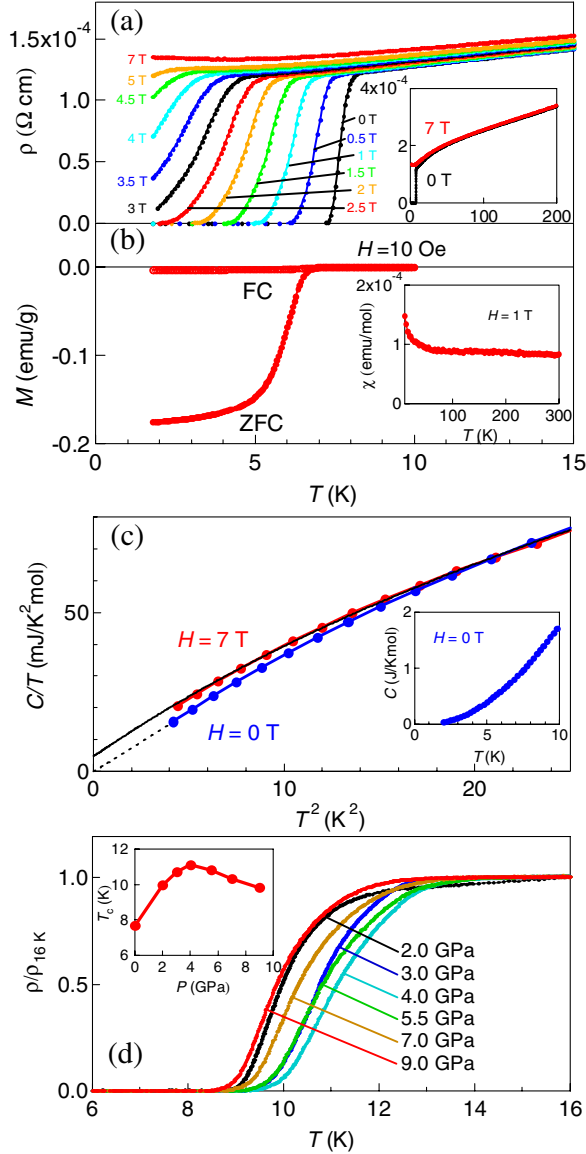


FIG. 3 (color online). (a) Temperature (T) dependence of the resistivity (ρ) under a magnetic field (H) applied perpendicular to the direction of the current. The inset shows ρ in a wider T range. (b) Magnetization (M) data at $H = 10$ Oe under zero-field-cooled (ZFC) and field-cooled (FC) conditions. The inset is the magnetic susceptibility (χ) in a normal state at $H = 1$ T. (c) Specific heat (C) divided by T at $H = 0$ and 7 T as a function of T^2 . The dotted line indicates the low T extrapolation. The solid line represents the results of the fitting (see text for details). The inset shows C in a wider T range. (d) ρ scaled by the 16 K value under high pressure (P). Note that the horizontal axis covers a limited T range near T_c . The inset shows the P dependence of the superconducting transition temperatures ($T_{c,s}$).

estimated as the midpoint of the superconductivity-normal metal transition; the values are plotted against T in Fig. 4(c). By extrapolating the data, we obtained the ground state value $H_{c2}(0) = 4.8 \pm 0.5$ T. According to the Bardeen-Cooper-Schrieffer theory [17], the H_{c2} value is related to the coherent length (ξ) as $H_{c2} = \phi_0/2\pi\xi^2$ (ϕ_0 being

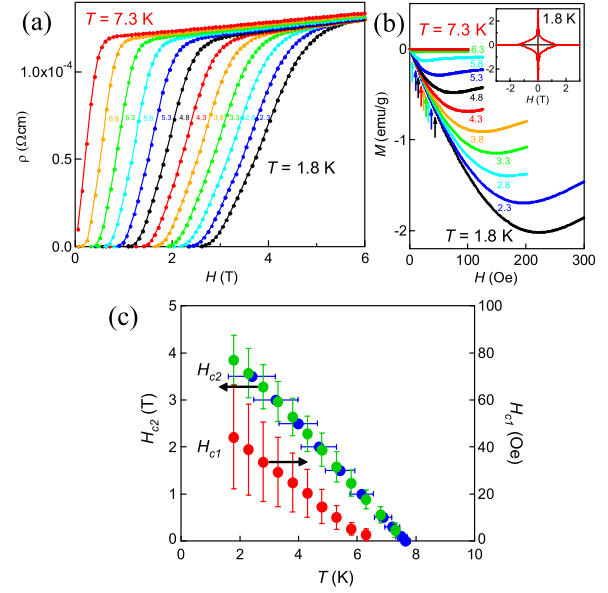


FIG. 4 (color online). (a) Magnetic-field (H) dependence of the resistivity (ρ) at fixed temperature (T). (b) Isothermal magnetization (M) curves at various values of T . The arrows indicate lower critical fields, where M deviates from a linear response. The inset shows an overall feature in a wider H range at 1.8 K. (c) T evolution of the upper and lower critical fields (H_{c2} and H_{c1} , respectively). The upper circles (blue and green, H_{c2}) are obtained from the resistivity data of fixed T and H scans, respectively. The lower circles (red, H_{c1}) are deduced from the M data.

the magnetic flux quantum). Using this formula, we get $\xi = 8.2$ nm. The magnetization isotherms shown in Fig. 4(b) exhibit typical type-II superconductor behavior. The lower critical field (H_{c1}), at which the magnetization deviates from a linear response [shown by arrows in Fig. 4(b)], are identified and are plotted as a function of T in Fig. 4(c). The ground state value is $H_{c1}(0) = 60 \pm 30$ Oe. The London penetration depth (λ) derived from the Bardeen-Cooper-Schrieffer formula $H_{c1} = (\phi_0/4\pi\lambda^2) \ln\lambda/\xi$ is 320 nm. The Ginzburg-Landau parameter ($\kappa = \lambda/\xi$) is 38, which is slightly larger than the value for $\text{Rb}_{0.23}\text{WO}_{3.02}$ [18].

In order to unravel the mechanism of high- T_c superconductivity in $\text{Hg}_{0.44}\text{ReO}_3$, we examined the normal-state properties. The magnetic susceptibility shows weakly T -dependent behavior [inset of Fig. 3(b)]; this can be well described by the sum of a T -independent Pauli paramagnetic susceptibility $\chi_P = 8.27 \times 10^{-5}$ emu/mol, and a contribution from localized impurity spins ($S = 1/2$ free spins with 0.16% of the sample). The C/T at 7 T, which is far above H_{c2} , approaches a finite value $\gamma = 4.9$ mJ/K² mol in the low T limit [Fig. 3(c)], where γ is the Sommerfeld coefficient. We computed the Wilson ratio $R_W = \pi^2 k_B^2 \chi_s / (3\mu_B^2 \gamma)$, where k_B is the Boltzmann constant, χ_s is the spin susceptibility, and μ_B is the Bohr magneton. This ratio is equal to one in a free Fermion gas and two in a strongly correlated Fermi liquid.

Assuming that the orbital susceptibility is negligible ($\chi_s = \chi_P$), $R_W = 1.23$. This clearly indicates that the electron correlation effect is not prominent in $\text{Hg}_{0.44}\text{ReO}_3$, ruling out the possibility of magnetic fluctuations acting as glue for the Cooper pairs.

Instead of the electron correlation effect, the importance of Hg-related phonons manifests itself through a close inspection of the lattice contribution to the specific heat. Even though the C/T deviates from a simple linear dependence on T^2 [Fig. 3(c)], we can roughly estimate the energy scale of phonons by fitting with $C = \gamma'T + \beta T^3$, where γ' and β are the fitting parameters. This fitting yields $\beta = 2.7 \text{ mJ/K}^4 \text{ mol}$. The β coefficient is related to the Debye temperature (θ_D) as $\beta = (12\pi^4/5)NR/\theta_D^3$, where N is the number of atoms per unit cell ($N = 4.44$) and R is the gas constant. $\theta_D = 147 \text{ K}$ in $\text{Hg}_{0.44}\text{ReO}_3$ is much lower than $\theta_D = 460 \text{ K}$ in ReO_3 [19], a compound that is also composed of corner-shared ReO_6 octahedra. This strongly hints at the existence of a low-lying phonon mode associated with Hg atoms. A more accurate analysis of C can be done as follows. We fit the data below 5 K with a three-components model $C = \gamma T + (12\pi^4/5)N_D R(T/\theta_D)^3 + 3N_E R \int_0^\infty dx g(x)(x/T)^2 \exp(x/T)/[\exp(x/T) - 1]^2$, where the first, second, and third terms represent contributions from the conducting electrons, the Debye phonon related to the ReO_3 framework, and the Einstein phonon related to Hg atoms, respectively. Here, we set $\gamma = 4.9 \text{ mJ/K}^2$, $N_D = 4$, $N_E = 0.44$, and $\theta_D = 460 \text{ K}$. We assume that the Einstein phonon energy shows a distribution due to the Hg vacancies according to the gamma distribution $g(x)$ with the mean θ_E and the variance $(\Delta\theta_E)^2$. As shown in the solid line in the Fig. 3(c), the fitting quality is fairly good when the fitting parameters are $\theta_E = 81 \text{ K}$ and $\Delta\theta_E = 45 \text{ K}$.

Corroborating evidence of such low-lying phonons comes from inelastic neutron-scattering experiments for $\text{Tl}_{0.33}\text{WO}_3$, where a dispersionless mode related to the vibration of Tl atoms in the large open tunnels is observed at 3.8 meV [20]. This type of phonon, which is sometimes called a rattling phonon, is also observed in compounds with a caged structure, such as filled skutterudites [21] and β pyrochlores [22,23]. A recent theoretical calculation revealed that rattling phonons induce a strong downward-concave T dependence of the resistivity [24]. Our resistivity data also exhibit a similar feature, where the crossover temperature from the upward- to downward-concave behavior to be $T^* \sim 10 \text{ K}$ [inset of Fig. 3(a)]. This suggests that electrons are strongly coupled with low-lying phonons. Therefore, we speculate that $(\text{Hg}_2)^{2+}$ polycation-related rattling phonons are relevant to the high- T_c superconductivity in $\text{Hg}_{0.44}\text{ReO}_3$. We point out the possibility that Hg 6s electrons, which are not fully bonded in the metal-metal bond, enhance the electron-phonon coupling.

To summarize, we have discovered a hexagonal bronze superconductor Hg_xReO_3 with the transition temperature

$T_c = 7.7 \text{ K}$, which is the highest among known hexagonal bronzes. The crystal structure has a unique aspect that open tunnels accommodate $(\text{Hg}_2)^{2+}$ polycations, the rattling of which is one candidate as an origin of the superconducting instability.

This work was supported by Special Coordination Funds for Promoting Science and Technology, Promotion of Environmental Improvement for Independence of Young Researchers, and Grant-in-Aid for Scientific Research (C) (No. 20550135). K. O. is grateful for support from the Special Postdoctoral Researcher's Program of RIKEN.

-
- [1] A. R. Sweedler, C. J. Raub, and B. T. Matthias, *Phys. Lett.* **15**, 108 (1965).
 - [2] A. R. Sweedler, J. K. Hulm, B. T. Matthias, and T. H. Geballe, *Phys. Lett.* **19**, 82 (1965).
 - [3] P. E. Biersted, T. A. Bither, and F. J. Darnell, *Solid State Commun.* **4**, 25 (1966).
 - [4] A. Magneli, *Nature (London)* **169**, 791 (1952).
 - [5] S. Raj *et al.*, *Phys. Rev. B* **77**, 245120 (2008).
 - [6] A. Hussain, R. Gruehn, and C. H. Ruscher, *J. Alloys Compd.* **246**, 51 (1997).
 - [7] L. Kihlberg and A. Hussain, *Mater. Res. Bull.* **14**, 667 (1979).
 - [8] P. Labbe, M. Goreaud, B. Raveau, and J. C. Monier, *Acta Crystallogr. Sect. E* **34**, 1433 (1978).
 - [9] K. Tatsumi, M. Hibino, and T. Kudo, *Solid State Ionics* **96**, 35 (1997).
 - [10] R. K. Stanley, R. C. Morris, and W. G. Moulton, *Phys. Rev. B* **20**, 1903 (1979).
 - [11] M. R. Skokan, W. G. Moulton, and R. C. Morris, *Phys. Rev. B* **20**, 3670 (1979).
 - [12] A. W. Sleight, T. A. Bither, and P. E. Biersted, *Solid State Commun.* **7**, 299 (1969).
 - [13] We also synthesized Hg_xReO_3 from a 1:1 molar ratio of HgO and Re, which results in considerable amounts of Re impurities. T_c of this sample is 8.0 K, which is slightly higher than $T_c = 7.7 \text{ K}$ of the sample grown from HgO and ReO_2 . The fact that a reducing atmosphere leads to a higher T_c markedly contrasts with the case of tungsten bronzes, where an acid etching increases T_c [J. P. Remeika *et al.*, *Phys. Lett. A* **24**, 565 (1967)].
 - [14] H. Taniguchi *et al.*, *J. Phys. Soc. Jpn.* **72**, 468 (2003).
 - [15] F. Izumi and T. Ikeda, *Mater. Sci. Forum* **321–324**, 198 (2000).
 - [16] For example, M. S. Schriewerpottgen and W. Z. Jeitschko, *Z. Anorg. Allg. Chem.* **620**, 1855 (1994).
 - [17] J. Bardeen, L. N. Cooper, and J. R. Schrieffer, *Phys. Rev.* **108**, 1175 (1957).
 - [18] L. C. Ting *et al.*, *Chin. J. Phys. (Taipei)* **45**, 237 (2007).
 - [19] F. C. Zumsteg and T. Pearsall, *Solid State Commun.* **16**, 751 (1975).
 - [20] W. A. Kamitakahara, K. Scharnberg, and H. R. Shanks, *Phys. Rev. Lett.* **43**, 1607 (1979).
 - [21] V. Keppens *et al.*, *Nature (London)* **395**, 876 (1998).
 - [22] K. Sasai *et al.*, *J. Phys. Soc. Jpn.* **76**, 104603 (2007).
 - [23] Y. Nagao *et al.*, *J. Phys. Soc. Jpn.* **78**, 064702 (2009).
 - [24] T. Dahm and K. Ueda, *Phys. Rev. Lett.* **99**, 187003 (2007).